SHOCK WAVE INDUCED FLOW SEPARATION CONTROL BY AIR-JET AND ROD VORTEX GENERATORS

FERNANDO TEJERO, PIOTR DOERFFER AND OSKAR SZULC

Institute of Fluid-Flow Machinery, Polish Academy of Sciences
Fiszera 14, 80-231 Gdansk, Poland

(received: 23 January 2015; revised: 25 February 2015;
accepted: 27 February 2015; published online: 3 April 2015)

Abstract: Flow separation control by Vortex Generators (VGs) has been analyzed over the last decades. The majority of the research concerning this technology has been focused on subsonic flows where its effectiveness for separation reduction has been proven. Less complex configurations should be analyzed as a first step to apply VGs in transonic conditions, commonly present in many aviation applications. Therefore, the numerical investigation was carried out for a Shock Wave-Boundary-Layer Interaction (SWBLI) phenomenon inducing strong flow separation at the suction side of the NACA 0012 profile. For this purpose, two kinds of VGs were analyzed: well documented Air-Jet Vortex Generators (AJVGs) and our own invention of Rod Vortex Generators (RVGs). The results of the numerical simulations based on the RANS approach reveal a large potential of this passive flow control system in delaying stall and limiting separation induced by a strong, normal shock wave terminating a local supersonic area.

Keywords: airfoil, boundary-layer, flow control, separation, shock wave, transonic conditions, vortex generator

1. Introduction

Flow control devices are designed to limit the boundary-layer growth and thus the flow separation. During the last decades, several active and passive flow control systems have been analyzed, such as: vortex generators [1], wall perforation [2] or synthetic jets [3]. Vortex generators are designed to create streamwise vorticity which induces an exchange of momentum in the direction normal to the wall. The transfer of high-momentum air towards the surface (into the low-momentum region) results in an increased wall shear stress, thus making the velocity profiles fuller and less prone to separation.

In the beginning of the 60s, Wallis *et al.* [4, 5] proposed the Air-Jet Vortex Generators (AJVGs) as an alternative to the classical Vane Vortex Generators

(VVGs). This flow control arrangement is implemented as an array of small orifices placed in a line transverse to the flow direction which produce streamwise vortices by the mixing between the jet blown from each orifice and the free-stream. The main advantage of the AJVGs is the absence of a parasite drag introduced by conventional VVGs due to their excessively large dimensions – height (h) of the order of the boundary-layer thickness (δ). A design of an effective AJVG for given flow conditions is challenging, mainly due to a large number of interrelated parameters under consideration, *i.e.*: the hole diameter (ϕ_{AJVG}) from where the air-jet is blown, the hole spacing (L) and the skew (α) and the pitch (θ) angles (see Figure 1).

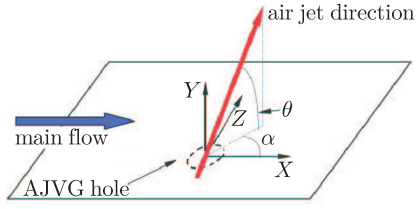

Figure 1. Schematic view of AJVG

It was in the 80s when Rao and Kariya [6] presented the low-profile vortex generators ($h/\delta < 0.625$) which have the potential of exceeding the performance of conventional VVGs ($h/\delta \approx 1$) due to a much lower parasite drag. Since that time, many researchers have investigated the influence of the shape of vortex generators for different applications (*e.g.* channel flows, airfoils, etc.). Table 1 summarizes the research focused on the improvement of the aerodynamic performance of airfoil/wing configurations by low-profile VGs. An extended state of the art on low-profile VGs has been presented by Lin recently [1].

Table 1. Summary of research on low-profile VGs [1]

Researcher	Test bed	VG type
Kerho [7]	Liebeck LA2573A airfoil	wishbones
Lin [8, 9]	3-element airfoil	trapezoidal vanes
Klausmeyer [10]	3-element airfoil	trapezoidal vanes
Ashill [11]	60° LE delta wing model	wires
Langan [12]	60° LE diamond wing model	co-rotating vanes
Ashill [13]	RAE 5243 transonic airfoil	counter-rotating vanes

The presented investigation is focused on an application of a new kind of a passive flow control system incorporating Rod Vortex Generators (RVGs) [14]. For rotorcraft configurations, vortex generators should operate permanently (hover [15]) or at well selected time intervals (forward flight [16, 17]). For instance, in case of helicopter rotor blades in high-speed forward flight, flow separation appears at the advancing side induced by Shock Wave-Boundary-Layer Interaction

(SWBLI) while a dynamic stall is present at the retreating side of the rotor disk due to the high inflow angle. For this reason, rods should be deployed only at certain times and hidden inside the blade for the rest of the rotation period. Since the technical complexity of the installation of a flow control system is of a primary importance, simpler RVGs are preferred over AJVGs. As for AJVGs, a similar set of parameters is necessary to design RVGs: rod diameter (ϕ_{RVG}), height (h), spanwise distance between devices (L) and skew (α) and pitch (θ) angles. Figure 2 presents a schematic view of a single, deployed RVG.

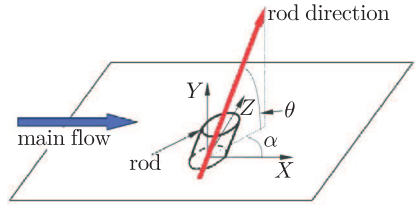

Figure 2. Schematic view of RVG

The proposed flow control devices (air-jet and rod vortex generators) have been already analyzed (experimentally and computationally) in channel flows proving their potential in separation control [18, 19]. A possible aerodynamic enhancement of a profile configuration by VGs is considered in the present paper as an initial step of the implementation for more complex applications (*e.g.* helicopter and wind turbine rotor blades). The classical NACA 0012 has been chosen for the research not only due to the large available experimental data base but preferably because it constitutes a basic cross-section of the Caradonna – Tung model rotor – a carefully chosen configuration for the implementation of RVGs [15–17]. The inflow Mach number was set to $\mathrm{Ma} = 0.8$ and the Reynolds number to $\mathrm{Re} = 9.0 \cdot 10^6$ (representative flow conditions commonly found at the advancing side of a helicopter rotor in high-speed forward flight). The reference case is validated against the experimental data of Harris [20], Ladson *et al.* [21, 22] and Mineck *et al.* [23]. Severe inflow conditions result in large extent of supersonic areas terminated by a strong shock wave which induces flow separation. The increase in the angle of attack (from 1.4° to 4.0°) provides even more severe conditions and stronger reverse flow. Comparison of polar graphs for both configurations (reference and flow control) confirms that the technology improves the aerodynamic performance of the NACA 0012 airfoil in transonic conditions near the maximum lift. In contrast to the conclusions drawn in the paper [24], it is proven numerically (and in accordance with [25]) that VGs are suitable candidates as transonic flow control devices aiming at reduction of separation.

2. Physical and numerical modeling

For the range of inflow conditions (see Table 2), the onset of separation appears for the angle of attack (AoA) equal to 1.4°. The strong shock wave induces

flow detachment that is expected to be controlled by streamwise vortex generators. The boundary-layer thickness (δ) directly upstream of the reverse flow location is approximately $0.01c$ (the chord is re-scaled to 1 m).

Table 2. Inflow conditions

Parameter	Value
Mach number, Ma [–]	0.8
Reynolds number, Re [–]	$9.0 \cdot 10^6$
angle of attack, AoA [°]	0.0° to 4.0°

According to the previous investigations of AJVGs conducted in the transonic wind tunnel of the Institute of Fluid-Flow Machinery, the diameter of the jet hole (ϕ_{AJVG}) should be of the order of 10%–20% of the boundary-layer thickness (δ) with a hole spacing following the ratio $L/\phi_{AJVG} = 10$ [18]. As a result of setting the jet hole diameter to $15\% \cdot \delta$ ($0.0015\,c$) the spanwise distance between AJVGs (L) was chosen to be equal to $0.015\,c$. On the other hand, an optimization process of the device suggested that the skew (α) and pitch (θ) angles of 65° and 30°, respectively, induced sufficiently strong streamwise vorticity (and therefore maximized the impact on the flow separation). The RVG design parameters were set according to the preliminary results obtained for channel flows [19]. The diameter of the rod vortex generator was kept with the same relation (L/ϕ_{RVG}) as for the jet hole of AJVGs (*i.e.* 10%–20% of δ), while the height (h) was set to $0.5 \cdot \delta$ (still within the definition of a low-profile VG according to Rao and Kariya). In this case, the optimization procedure of the skew and pitch angles suggested 45° and 30°, respectively. Table 3 summarizes the designed parameters of both flow control systems considered in the present research.

Table 3. Design parameters of AJVGs and RVGs

Parameter	AJVGs	RVGs
diameter, ϕ [c]	0.15%	0.15%
spacing, L [c]	1.5%	1.5%
height, h [c]	–	0.5%
skew angle, α [°]	65	45
pitch angle, θ [°]	30	30

Three, 3d block structured computational grids were prepared for the present simulations: reference (no flow control), AJVGs and RVGs. The meshes were generated semi-automatically using a python based internal programming language embedded within the Interactive Grid Generator (IGG) – commercial Numeca International software. It is evident that a large number of vortex generators (approximately 230 for the full model employed by Harris [20]) is required to cover the whole span multiplying the required computer resources enormously. Moreover, the grid density in the vicinity of vortex generators and

longitudinal vortices requires a sufficient spatial resolution, even in case of the RANS modeling. Therefore, the computational domain was restricted down to a slice with a single vortex generator and employing the translational periodicity boundary condition in the spanwise direction. Still, the remaining task was computationally very demanding, mainly due to the complexity of the flow structures simulated. A C-type grid was applied for all computations. The non-dimensional distance of the first layer of cells from the solid surface of the blade y^+ was of the order of 1. Although, the topology was slightly modified for the RVG set-up, the spacings and the number of volumes were kept almost constant in order to compare the flow structures between the three studied cases (minimizing the grid influence). Table 4 summarizes the final number of blocks and volumes of the meshes used for the present CFD study aiming at the reduction of flow separation at the NACA 0012 airfoil by means of streamwise vortex generators.

Table 4. Computational grids

Configuration	Number of blocks	Number of volumes
Reference	26	$5.48 \cdot 10^6$
AJVG	31	$5.51 \cdot 10^6$
RVG	47	$5.28 \cdot 10^6$

Figure 3 presents the mesh topology for the AJVG computational grid. The vicinity of the jet tube is resolved with a butterfly arrangement which is extended up to the far-field (located at $50\,c$). From the technical point of view the outlets of AJVGs should be connected by internal ducts with the inlet of air located close to the stagnation point of the flow. An increase in the angle of attack

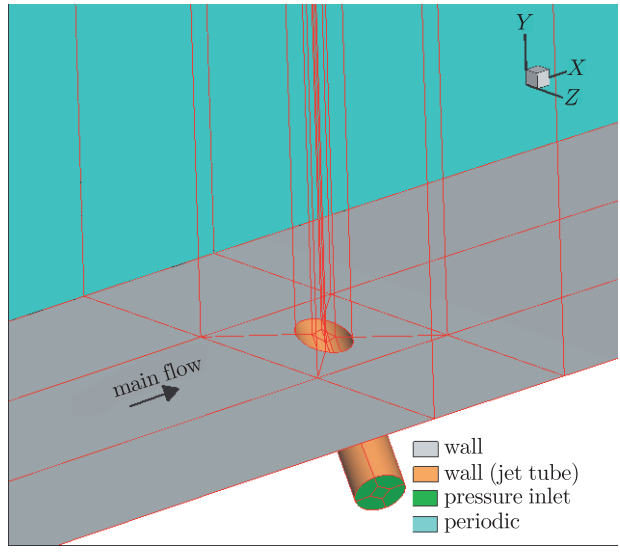

Figure 3. Grid topology and boundary conditions for AJVG

shifts the stagnation point, thus requiring a modification of the numerical model (computational grid). To simplify the approach it is only the outlet jet tube of the AJVG that is retained at the suction side, below the surface of the airfoil, keeping the connection with the stagnation point by setting the total pressure and temperature boundary condition at the bottom with values equal to the main stream parameters. With the proposed method it is sufficient to construct only a single numerical mesh suitable for all flow incidences. The reference mesh (no control) is created by removing all computational blocks of the jet tube allowing a direct comparison of results without artificial grid influence. Figure 4 presents a similar grid topology designed for a single RVG with the butterfly blocking at the top of the rod.

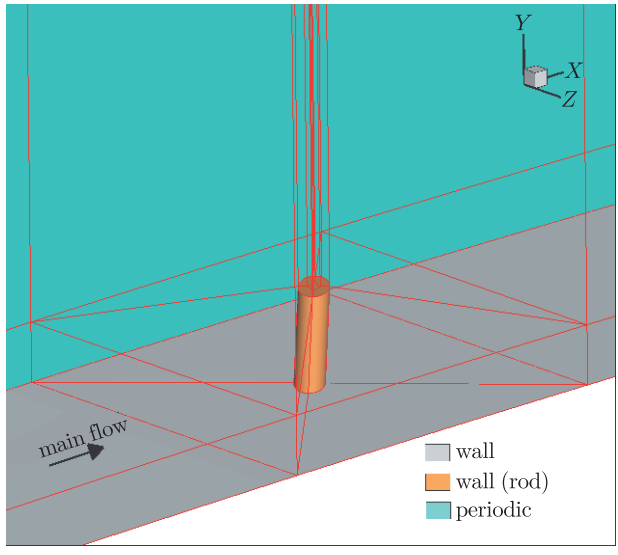

Figure 4. Grid topology and boundary conditions for RVG

For the reference case (no control) a no-slip wall boundary condition (b.c.) with zero heat-flux (adiabatic) is applied at the surface of the airfoil. The outer edges of the computational domain are treated as subsonic far-field. Instead of the usual setting of symmetry for 2d airfoils, the translational periodicity b.c. models a row of infinite numbers of VGs. For the flow control configurations, the AJVG and RVG surfaces are treated as no-slip walls as well, except for the bottom of the jet tube where the total pressure and temperature condition mimic a connection with a stagnation point.

The present work was carried out with a block structured CFD code Fine/Turbo from Numeca International. The physical modeling was based on the Reynolds-Averaged Navier-Stokes (RANS) equations closed by the Spalart-Allmaras turbulence model [26], a combination proving excellent speed and stability. The system of differential equations was closed by a perfect gas model. The viscosity value was calculated according to the Sutherland's law. The numer-

ical algorithm used a semi-discrete approach with a finite volume central scheme for spatial discretization and Runge-Kutta type integration of time. The CFL number was set to 2. A full multigrid strategy was implemented to improve the convergence rate. For each simulation a drop of residuals of 6.5 orders of magnitude ensured convergence of forces and moments (lift, drag and pitching moment coefficients).

3. Numerical results and discussion

3.1. Reference case (no control)

A strong shock wave-boundary-layer interaction leading to flow separation at the NACA 0012 airfoil was computed ($\mathrm{Ma} = 0.8$ and $\mathrm{Re} = 9.0 \cdot 10^6$) and compared against the experimental data gathered by Harris [20], Ladson *et al.* [21, 22] and Mineck *et al.* [23]. The pressure coefficient C_p distributions available in the Harris data were analyzed as well. The data of Harris, Ladson and Mineck was corrected for wall interference effects and the presence of slots in the wind tunnel floor and ceiling. The comparison of the CFD result and measured aerodynamic characteristics for the proposed flow conditions is presented in Figure 5. It is evident that transonic experiments are very sensitive to the details of the wind tunnel set-up resulting in a noticeable scatter of the measured data. During the experiments a transition location from laminar to turbulent was triggered at $5\%\,c$, while the computations were performed in a fully turbulent mode. There is an acceptable agreement of the normal force coefficient C_n polar which fits well with the available experimental data. The comparison of the drag force coefficient C_d

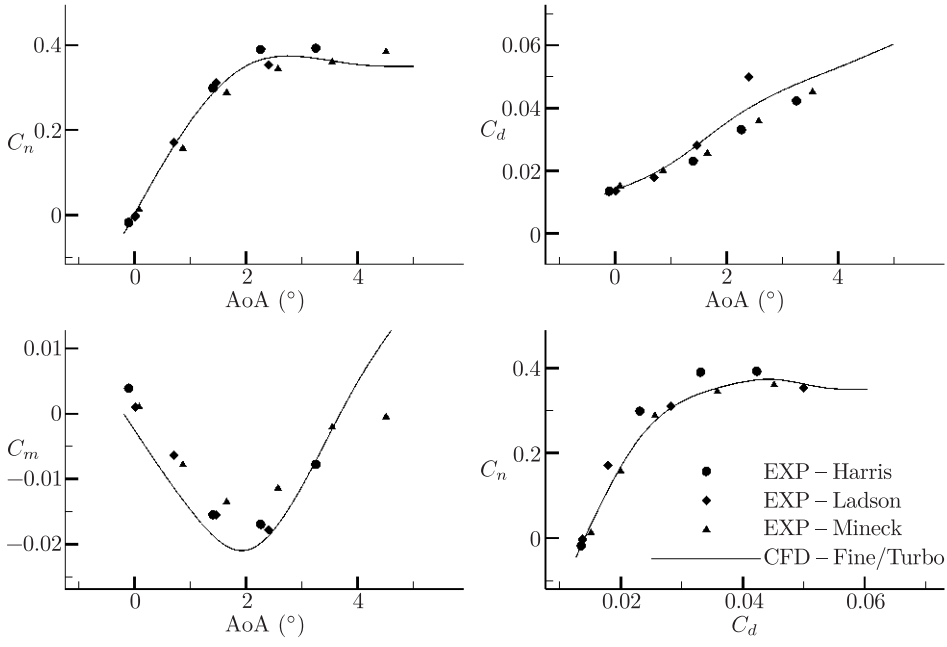

Figure 5. Aerodynamic characteristics of the NACA 0012 profile ($\mathrm{Ma} = 0.8$ and $\mathrm{Re} = 9.0 \cdot 10^6$)

is satisfactory for all the angles of attack as well. CFD overestimates the C_d with respect to the experimental data. The accurate prediction of the pitching moment coefficient C_m is challenging due to its sensitiveness to the position of the shock wave. For this reason, the obtained comparison is acceptable since the shape of the experimental curve is well reproduced.

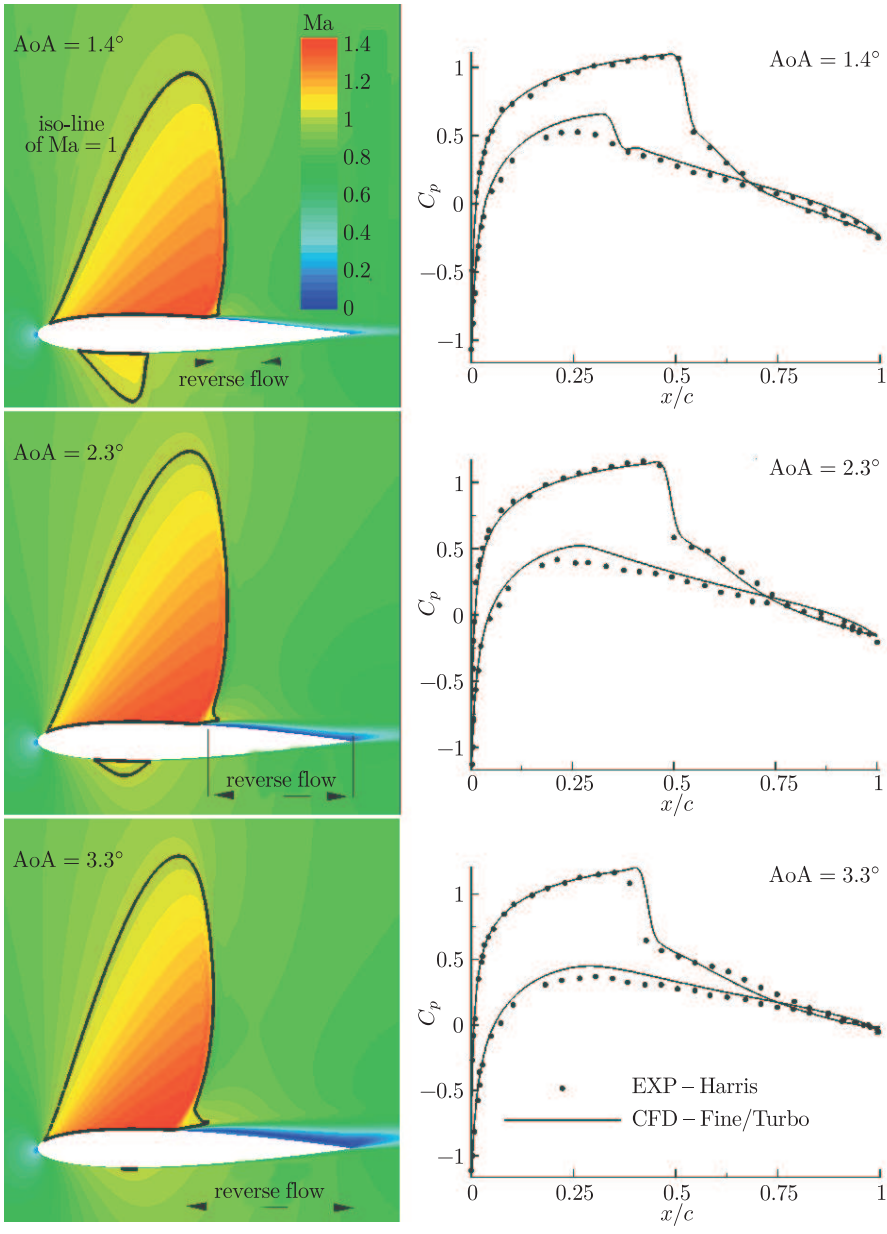

Figure 6. Contour map of Mach number and pressure distributions for the NACA 0012 profile (Ma = 0.8, Re = $9.0 \cdot 10^6$ and AoA = 1.4°, 2.3° and 3.3°)

Figure 6 presents a contour map of the Mach number and the pressure coefficient C_p distribution for three inflow angles of 1.4°, 2.3° and 3.3°. Usually, the shock wave moves upstream when the incidence is increased and the flow separation follows the compression. The normal shock wave location for AoA = 1.4° is well reproduced by the numerical simulation (a simulated weak shock at the pressure side is not present in the measurements). With an increased angle of attack up to AoA = 2.3° the prediction of the shock wave position is still acceptable for such severe conditions. The separation bubble grows with respect to the previous case due to stronger shock wave-boundary-layer interaction. For the last inflow angle computed (AoA = 3.3°) the shock wave is slightly shifted downstream of the measured position but still with a satisfactory correlation. The reason for this difference may be connected with an assumption of the steady flow not present in reality due to severe buffeting initiating above AoA = 2.3° and the given flow conditions [27].

3.2. Flow control cases (AJVG and RVG)

Five angles of attack are considered: AoA = 1.4°, 2.3°, 3.3°, 3.5° and 4.0° with the location of the flow detachment point in the symmetry plane at $x/c = 0.57$, 0.55, 0.48, 0.45 and 0.40, respectively. The angle of attack of 1.4° is considered as the onset of separation. The reverse flow is limited by the reattachment line. On the other hand, for AoA = 2.3° the flow is detached until the trailing edge. The other AoAs = 3.3°, 3.5° and 4.0° are investigated to prove the positive impact of the flow control devices near the maximum lift of the airfoil. The shift of the initial detachment line with the increasing incidence implies that it is necessary to study the flow control location with respect to the onset of separation. This parameter (a key factor in reaching optimum performance) is still under investigation. The flow control device should be neither positioned next to the flow separation (not enough space to develop vortical structures), nor far away (diffused vorticity). The best location of the AJVG hole (for the given flow conditions) was investigated in the past [28]. The position at $x/c = 0.30$ provided the best ratio of lift to drag for the investigated range of AoA. Similar positions of AJVGs and RVGs with respect to the separation zone were considered for the numerical study. Due to the insertion of vortex generators, emerging, high streamwise vorticity areas modify the boundary-layer profile depending on the value of skew and pitch angles of the air-jet and rod (Figure 7).

Figures 8 and 9 present hypothetical contour maps of the skin friction coefficient C_f and the surface streamlines over the suction side of the NACA 0012 profile for the reference, AJVG and RVG cases, respectively. Reattachment is observed for AoA = 1.4° (Figure 8), while the separation extends down to the trailing edge for the AoA = 4.0° (Figure 9). The negative value area of skin friction increases with the angle of attack (due to a stronger reverse flow). When the flow control technique is applied, longitudinal zones of increased C_f are formed delaying the boundary-layer separation. Although a single vortex generator is modeled with periodic conditions, a set of 4 vortex generators is analyzed (total

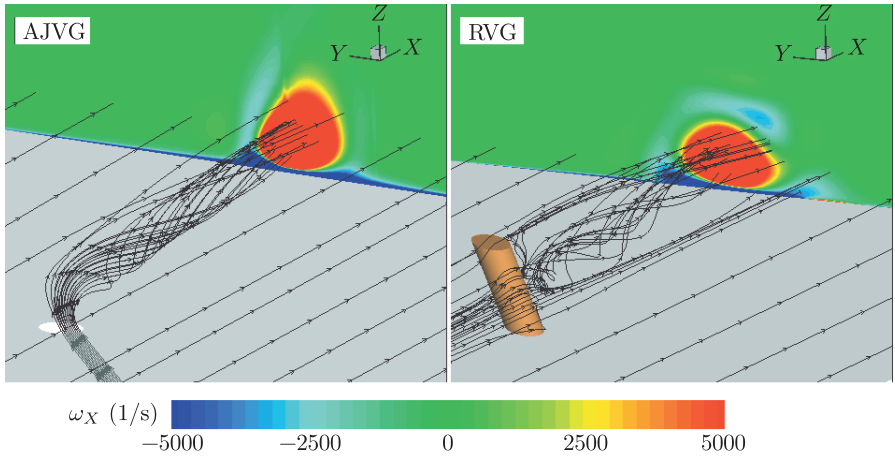

Figure 7. Streamwise vortex generation by means of AJVG (left) and RVG (right)

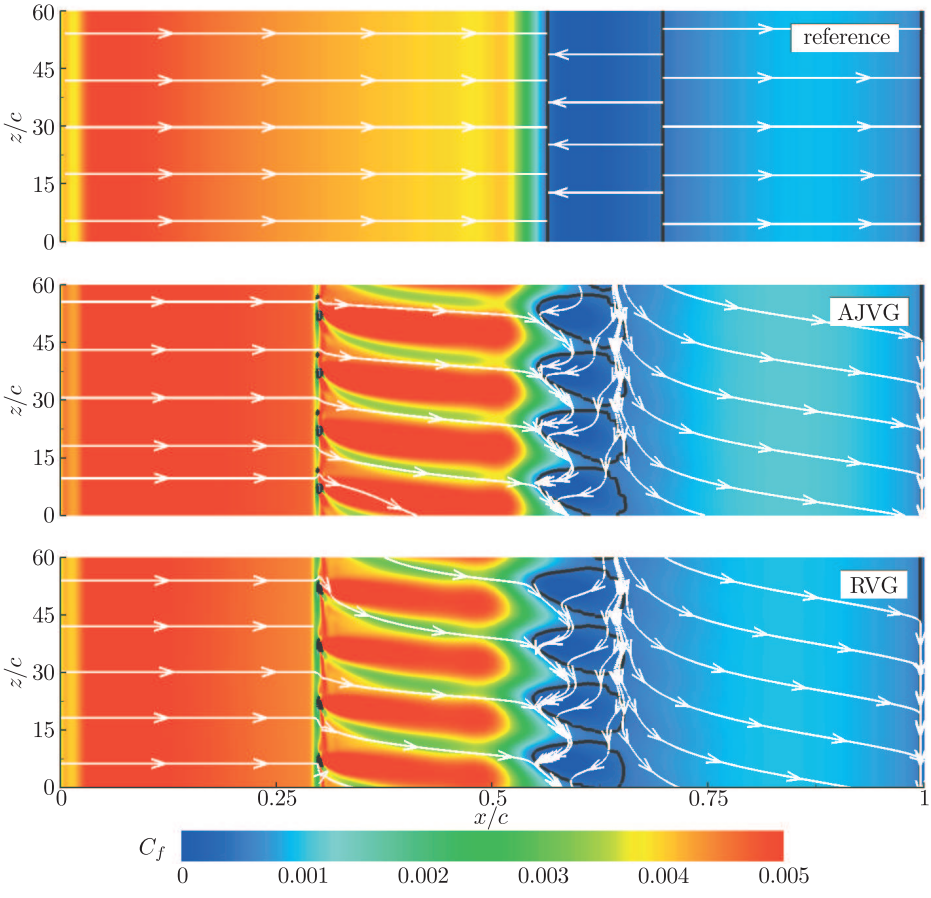

Figure 8. Friction coefficient C_f and streamlines (Ma = 0.8, Re = $9.0 \cdot 10^6$, AoA = 1.4°)

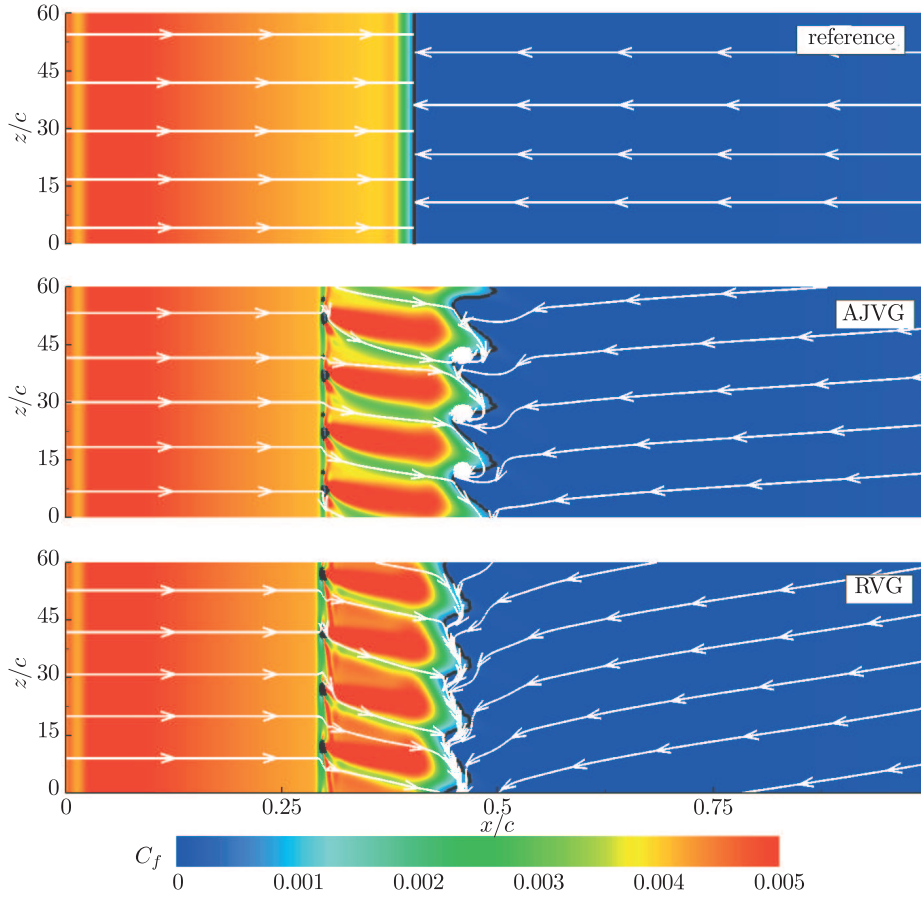

Figure 9. Friction coefficient C_f and streamlines ($\mathrm{Ma} = 0.8$, $\mathrm{Re} = 9.0 \cdot 10^6$, $\mathrm{AoA} = 4.0°$)

span of $0.06\,c$) for visualization purposes and assessment of the level of interaction between the flow control techniques (AJVG or RVG). For the $\mathrm{AoA} = 1.4°$ the flow separates at approximately $0.55\,c$ and reattaches at $0.70\,c$. With the AJVG, the same location of flow detachment is maintained with a more upstream reattachment at a mean value of $0.65\,c$ while approximately the same reattachment position is obtained with RVGs. It is observed that high vorticity areas are induced by AJVGs and RVGs downstream of the flow control device location and upstream of the flow separation but there is no evidence of any vortex pattern present downstream of the reattachment line. The same behavior is pointed out in publications presenting experimental results for VGs (*e.g.* [25]) indicating that either the longitudinal vortices are lifted over the interaction by the separation bubble or dissipated by the unsteady processes occurring in the mixing region. Similar behavior is present in the numerical results, however, it is not clear if the main mechanism behind is the physical or numerical dissipation of the vortex. When the angle of attack is increased above 2.0°, the flow separation is strong enough to prevent reattachment to the wall.

The surface streamlines are deflected and increased friction zones are developing, reaching the separation bubble. The application of vortex generators does not assure full reattachment of the flow (weak vortices) but the detachment line is shifted downstream (as well as the skin friction coefficient value is increased). For AoA = 4.0°, the detachment line for the reference case is located at $0.40\,c$. The application of AJVGs delays the separation line to $0.45\,c$, while the RVGs shift the onset of separation to $0.44\,c$ (reduction of the separation length of 4%–5% c).

Figure 10 presents the influence of the AJVG and RVG application on the normal force C_n, drag C_d and pitching moment C_m coefficient polars. Since the onset of separation is present at AoA = 1.4°, no improvements are expected for lower incidences. When the reverse flow develops, the streamwise vorticity is effectively reducing it, thus improving the aerodynamic performance of the profile in terms of C_n. The application of the flow control system delays the stall angle of the airfoil by 2.0°. Unfortunately, the increment of lift (normal force) is ligated to a drag penalty for higher angles of attack. The comparison of the normal force to the drag ratio C_n/C_d confirms that both flow control devices improve the aerodynamic performance of the NACA 0012 airfoil in transonic conditions. When AoA is less than 3.0° the shape of the C_m polar is identical between all the 3 cases considered (reference, AJVG and RVG). A noticeable difference is visible only for the largest separation size present for AoA = 4.0°.

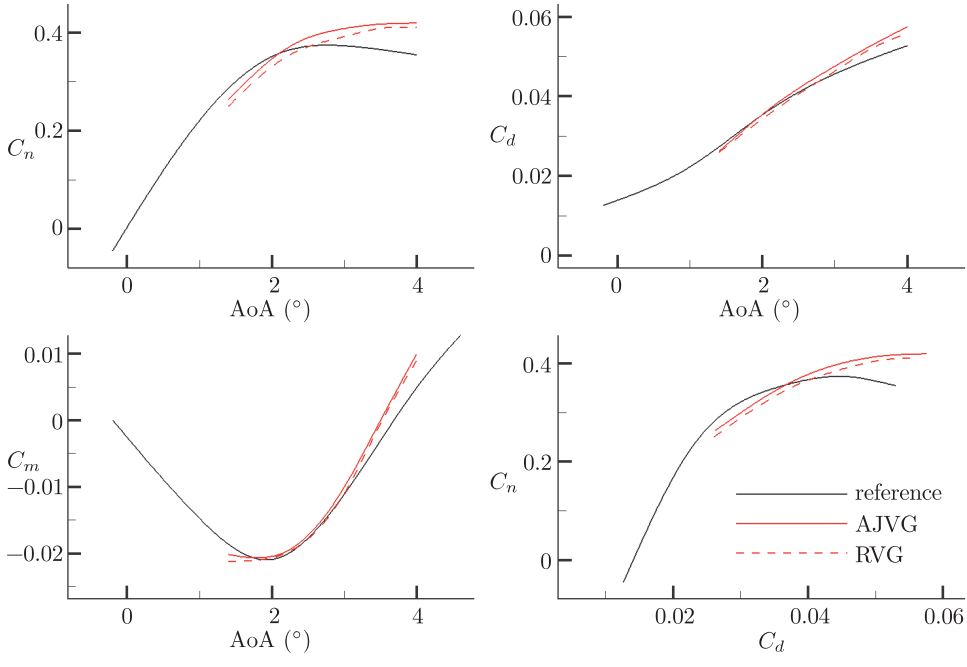

Figure 10. Comparison of normal C_n, drag C_d and pitching moment C_m coefficients (Ma = 0.8 and Re = $9.0 \cdot 10^6$)

4. Conclusions

Two passive flow control systems were analyzed in transonic conditions: Air-Jet Vortex Generators (AJVGs) and Rod Vortex Generators (RVGs). The numerical model for the reference case (no flow control) was validated against the available experimental data. The severe flow conditions were properly reproduced by numerical simulations. It was proved that the existing flow separation caused by the shock wave-boundary-layer interaction on the NACA 0012 airfoil was reduced by streamwise vorticity. The efficiency of air-jet vortex generators (the method suggested in the literature) and rod vortex generators (the authors' own method) was analyzed and compared for a range of angles of attack. It was concluded that both methods were promising candidates limiting massive flow separation (near stall angle). Since AJVGs and RVGs are designed for more complex configurations (e.g. helicopter rotor blades), it is important to study the difficulties of the technical implementation. For angles of attack above 3.0°, there is a strong buffet present in experiments not resolved by CFD. In the next step, this phenomenon is to be studied and the influence of AJVGs and RVGs in terms of the buffet onset is to be analyzed.

Acknowledgements

This work was supported by the 7$^{\text{th}}$ Framework Programme project IMESCON (Grant Agreement PITN-GA-2010-264672). This research was supported in part by the PL-Grid Infrastructure and TASK Supercomputing Center in Gdansk.

References

[1] Lin J C 2002 *Progress in Aerospace Sciences* **38** 389
[2] Doerffer P and Szulc O 2011 *Journal of Engineering Systems Modelling and Simulation* **3** (1–2)
[3] Rimasauskiene R, Matejka M, Ostachowicz W, Kurowski M, Malinowski P, Wandowski T and Rimasauskas M 2014 *Mechanical Systems and Signal Processing* **50-51** 607
[4] Wallis R A 1960 *A preliminary note on a modified type of air jet boundary layer control*, *Aeronautical Research Council*, Rept. CP 513
[5] Wallis R A and Stuart C M 1962 *On the control of shock-induced boundary layer separation with discrete air jets*, *Aeronautical Research Council*, Rept. CP 595
[6] Rao D M and Kariya T T 1988 *Boundary-layer submerged vortex generators for separation control – an exploratory study*, Proceedings of the AIAA, ASME, SIAM and APS National Fluid Dynamics Congress 839
[7] Kerho M, Hutcherson S, Blackwelder R F and Liebeck R H 1993 *Journal of Aircraft* **30** (3) 315
[8] Lin J C 1999 *Control of turbulent boundary-layer separation using micro-vortex generators*, *AIAA Paper*, 99-3404
[9] Lin J C, Robinson S K, McGhee R J and Valarezo W O 1994 *Journal of Aircraft* **31** (6) 1317
[10] Klausmeyer S, Papadakis M and Lin J C 1996 *A flow physics of study of vortex generators on a multi-element airfoil*, *AIAA Paper*, 96-0548
[11] Ashill P R and Riddle G L 1994 *Control of leading-edge separation on a cambered delta wing*, *AGARD Report*, CP-548

[12] Langan K J and Samuels J J 1995 *Experimental investigation of maneuver performance enhancements on an advanced fighter/attack aircraft*, *AIAA Paper*, 95-0442
[13] Ashill P R, Fulker J L and Hackett K C 2001 *Research at DERA on sub boundary layer vortex generators (SBVGS)*, *AIAA Paper*, 2001-0887
[14] Doerffer P, Flaszyński P and Szwaba R 2009 *Polish Patent P. 389685*
[15] Doerffer P, Szulc O, Tejero Embuena F L and Martinez Suarez J 2014 *eScience on Distributed Computing Infrastructure. Achievements of PLGrid Plus Domain-Specific Services and Tools*, Bubak M, Kitowski J and Wiatr K (eds.), Springer, **8** 429
[16] Tejero Embuena F L, Doerffer P and Szulc O 2014 *Journal of Physics: Conference Series* **530** (1) 12067
[17] Tejero Embuena F L, Doerffer P and Szulc O 2015 *Application of passive flow control device on helicopter rotor blades*, *Journal of the American Helicopter Society* (accepted)
[18] Doerffer P, Hirsh C, Dussauge J P, Babinsky H and Barakos G N 2010 *Unsteady effect of shock wave induced separation. Notes on Numerical Fluid Mechanics and Multidisciplinary Design*, Springer
[19] Flaszyński P and Tejero Embuena F L 2013 *RANS numerical simulation of effectiveness of vortex generators in a curved wall nozzle*, *IMP PAN Report No. 365/2013* (in polish)
[20] Harris C D 1981 *Two-dimensional aerodynamic characteristics of the NACA 0012 airfoil in the Langley 8-foot transonic pressure tunnel*, *NASA Technical Memorandum*, 81927
[21] Ladson C L, Hill A S and Johnson G Jr 1987 *Pressure distributions from high Reynolds number transonic tests of an NACA 0012 airfoil in the Langley 0.3-meter transonic cryogenic tunnel*, *NASA Technical Memorandum*, 100526
[22] Ladson C L and Hill A S 1987 *High Reynolds number transonic tests of an NACA 0012 airfoil in the Langley 0.3-meter transonic cryogenic tunnel*, *NASA Technical Memorandum*, 100527
[23] Mineck R E and Hartwich P M 1996 *Effect of full-chord porosity on aerodynamic characteristics of the NACA 0012 airfoil*, *NASA Technical Paper*, 3591
[24] Krzysiak A 2008 *AIAA Journal* **46** (9) 2229
[25] Souverein L J and Debieve J F 2010 *Effect of air jet vortex generators on a shock wave boundary layer interaction*, *Experiments in Fluids* **49** 1053
[26] Spalart P R and Allmaras S R 1992 *A one-equation turbulence model for aerodynamic flows*, *AIAA-92-0439*
[27] McDevitt J B and Okuno A F 1985 *Static and dynamic pressure measurements on a NACA 0012 airfoil in the Ames High Reynolds Number Facility*, *NASA Technical Paper*, 2485
[28] Tejero Embuena F L, Doerffer P and Szulc O 2013 *Effect of passive air jet vortex generator on NACA 0012 performance*, *Proceedings of the 5th European Conference for Aeronautics and Space Sciences*